Experimental study of an ocean surface cleaning system

Chun-Yan Ji[a], Jian-Ting Guo[a], Ren-Chuan Ye[a*], Qi-Lin Yin[a], Wei-Yao Xu[a], Zhi-Ming Yuan[b]

[a]School of Naval Architecture and Ocean Engineering, Jiangsu University of Science and Technology, Zhenjiang, 212100, China

[b]Department of Naval Architecture, Ocean and Marine Engineering, University of Strathclyde, Glasgow, UK

Abstract

This paper presents a novel design of an ocean surface cleaning system (OSCS), which can be operated at various sea sites. The system weathervanes around the mooring system, so that the marine debris can be effectively concentrated by the OSCS. In order to verify the technical feasibility and efficiency of this novel OSCS, a series of experiments in a wave tank were conducted. The prototypes and metocean data were designed to clean marine debris at Ningbo Xiangshan Port. From the statistics of the testing results, it is found that the novel OSCS can effectively concentrate and clean marine debris of different types. We also measured the hydrodynamic responses of the OSCS under various sea conditions. The results show that the system's motion responses in the vertical plane are small, indicating the marine debris could not escape from the top and bottom of the system. Meanwhile, the motions in the horizontal plane are sufficiently high to cover a large ocean surface area. The present study indicates that the novel OSCS can be used to clean a large ocean surface at high efficiency.

Keywords: Ocean surface cleaning system (OSCS); Marine debris; Collection efficiency; Hydrodynamic assessment.

1. Introduction

With the continuous upgrading of offshore marine structures at the design and manufacturing level, a wider range of coastline and sea activities are being conducted, and marine debris is proliferating at an increasing rate. Global plastic trash production in quantity has been increasing every year. From 1950 to 2007, the world's total population increased from 2.7 billion to 7 billion, and the mass of plastic products increased from 1.5 million tons per year to 270 million tons per year[1]. According to data released by Eurostat, in 2012 alone, 288 million tons of plastic products were produced globally[2], which is close to the total weight of all humans[3]. Only about 9% of plastic trash can be recycled. Marine plastic trash causes huge economic losses to the environment of the marine ecosystem. In recent years, as the results of studies on the potential impact of plastics on marine ecosystems have been gradually disclosed, public attention to towards marine plastic trash has increased[4, 5]. In 2015, the research team from the University of Georgia in the United States investigated the amount of plastic trash produced in 192

coastal countries. Statistics published in the journal "*Science*" showed that the world's annual ocean plastic trash mass was between 4.8 million and 12.7 million tons[6]. In 2018, the National Oceanic and Atmospheric Administration (NOAA) released an annual Arctic report that pointed out that in the past 10 years, marine debris, mainly plastic debris, increased by 20 times in the Arctic Ocean. According to current production trends and usage patterns, if plastic trash management and infrastructure are not further improved, pollution of marine plastic trash may triple by 2025 compared to 2015, reaching about 155 million tons, and by 2050, and the weight of the ocean plastic debris in the fish will exceed that of the fish[7], and almost all seabirds will accidentally eat plastic trash[8].

At present, marine debris cleaning work is mainly done by "marine debris cleaning ships". These ships cruise offshore, letting seawater pass through their built-in filters, collecting filtered plastics and other marine debris[9]. This method is inefficient and expensive, and is usually only used in trash accumulation zones, such as ports, while marine debris scattered in the open sea is difficult to clean up effectively. According to different marine debris collection types, water surface trash collection equipment is mainly divided into conveyor type, bucket type, rotary type and grab type. RanMarine Technology Co., Ltd. designed a marine debris cleaning system called "Waste Shark"[10], which is 10 meters long and 4 meters wide, its maximum continuous operation time is 10 hours, its service life is 15 years, and its maximum daily marine debris collection mass is 500kg. As for the cleaning of marine debris in small aquatic areas, operation requirements are also high for sea conditions. Ruangpayoongsak et al.[11] designed a catamaran-based trash cleaning device, which added a conveyor belt in the middle of the catamaran, and added waste collection nets on both sides of the catamaran, and recycled trash to the catamaran using a robotic arm, as verified by experiments. Zhongli Wang et al.[12] designed marine debris cleaning equipment based on a quadrimaran, whose recovery equipment is a conveyor belt. Zhang H T et al.[13] designed a new type of processing equipment based on a catamaran and conducted strength analysis.

In addition to the above conventional trash collection equipment, many passive marine debris collection equipment have been invented in recent years. Boyan Slat has made it his mission to remove plastic from the rivers and oceans. His organization, The Ocean Cleanup, has successfully started to clean the pollution that has been circling in the Great Pacific Garbage Patch and many main rivers. The "Interceptor" marine debris cleaning equipment is mainly used to clean up marine debris in inland rivers, but at the same time, it can also effectively prevent floating trash from rivers flowing into the sea. The

"Interceptor" has been updated to the fourth generation, which is 24 meters long and 8 meters wide, and 5 meters high, and all the energy for the operation is provided by solar energy[14]. Boyan Slat and his team designed System 001, System 001/B, and System 002, which are the world's first cleanup systems to be trialed and utilized in the Great Pacific Garbage Patch–the world's largest accumulation zone of ocean plastics, situated halfway between Hawaii and California[15]. In 2020, the Offshore Mechanics and Arctic Engineering International Conference (OMAE); listed the study of the dynamics of marine debris and its clean-up as one of the areas of high concern in the field of ocean engineering in the future[16]. ISOPE2020 (International Society of Offshore and Polar Engineers) opened up a special symposium discussing marine debris[17].

To conclude, contemporary water surface marine debris cleaning equipment is still not efficient, the current marine debris cleaning equipment is mainly used in rivers, and this technology is immature for open sea areas. This paper designed a new type of passive ocean surface cleaning system (OSCS), which is mainly used for open sea areas. The marine debris collection efficiency and hydrodynamic performance of the OSCS are studied in detail by a series of model tests. The equipment has the following advantages: 1) it can be arranged in open sea areas by the mooring system and is suitable for the marine debris accumulation zone in open water areas; 2) the equipment has mobility and can be deployed in different sea areas by move the mooring system; 3) the equipment has a simple structure and high marine debris cleaning efficiency; 4) in comparison with domestic and foreign research, the equipment has strong innovation and engineering application prospects.

2. Design of OSCS

2.1 Concept design

Ningbo City has invested millions of yuan to clean-up marine debris in coastal waters (**Fig.1**). The tool of choice for marine debris cleaning is still traditional manual boat fishing, which has low efficiency, high cost and, involves extremely hard work for salvage workers. This paper develops a new concept design of OSCS to clean marine debris cleaning at Ningbo Xiangshan Port.

The new OSCS includes the following important properties: 1) environmentally friendly; 2) removability; 3) automatic collection; 4) low maintenance needs; 5) high strength. A new type of OSCS is designed based on the above-mentioned design concept, which is mainly composed of floating body, connecting structure, marine debris collection net and supporting structure (**Fig.2**). The stabilizing pontoon is fixed to the main body of

the ultra-long floating body; the marine debris collection net is installed between two adjacent single-section floating bodies. The main body of the ultra-long floating body is equipped with a mooring system, which is installed in open sea areas by the mooring system, and it is suitable for the marine debris accumulation zone in offshore waters. The main body of the OSCS is formed by connecting several single-section floating bodies in sequence, and the overall equipment is arc-shaped. Each single-section floating body is composed of a buoy and connectors on both sides of the buoy. The connector is composed of four circular rods (the four circular rods are separated by 90 degrees) and the horizontal fixed structure at intervals on the circular rods. Each single-section floating body has a certain arc, and different single-section floating bodies are connected to form arc-shaped OSCS. As shown in **Fig.2**, a mesh bag is installed at the opening of the trash cleaning equipment. The mesh bag is used to collect marine debris that passes through the floating body, which is optimized based on the actual marine debris statistics. The mesh bag in the middle is the largest in size and the mesh bags on both sides decrease in size gradually.

Fig.1 Marine debris on the sea surface of Xiangshan Port[18]

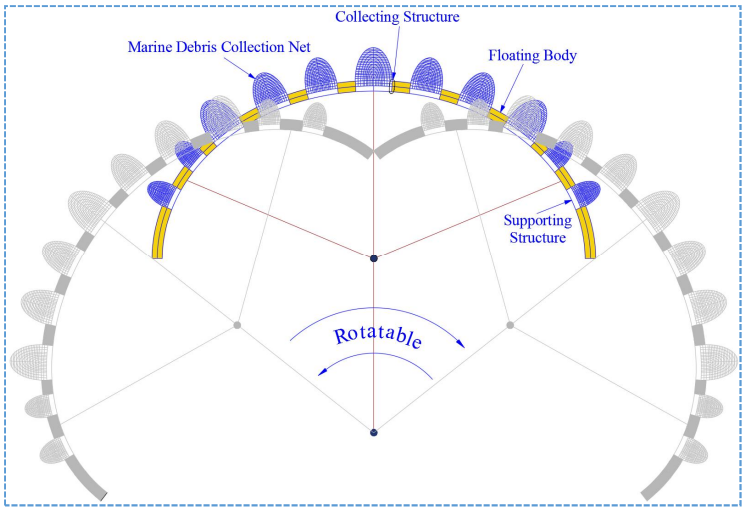

Fig.2 Concept design sketch of new ocean surface cleaning system (OSCS)

2.2 Design case

2.2.1 Sea conditions at Xiangshan Port

Marine debris distribution, waves and currents have an important effect on the hydrodynamic performance and trash collection efficiency of cleaning equipment. A new type of OSCS is designed according to the marine debris cleaning needs of Ningbo Xiangshan Port. There are six horizontal islands outside Xiangshan Port for cover, and the influence of sea waves on the harbor area is small, and it is mainly affected by local wind and waves. The water area in the middle and top of the harbor area is small, and there are many islands in the bay. The terrain is complex, but the water cover condition is good. In general, the harbor area is flat, and the waves are small. When the north bank is affected by a southerly wind, the maximum wave height ($H_{1/10}$) is about 1.8 m, and the average wave period is T = 4.8 s. When the south bank is affected by a northerly wind, the maximum wave height ($H_{1/10}$) is about 1.7 m, and the average period T is 4.7 s. Xiangshan Port has little influence from the wind and the waves, and is a well sheltered harbor. The actual wave and current distributions are listed in **Tab.1** according to wave and current monitoring condition.

Tab.1 Actual wave and current distribution in Xiangshan Port

Condition name	Actual conditions		
	Wave high(m)	Current(m/s)	Period(s)
A	0.2	0.4	4.472
B	0.5	0.8	6.708
C	0.7	1.0	--
D	1.0	1.2	--
E	1.5	1.6	--
F	2.0	--	--

2.2.2 Type and size of marine debris in Xiangshan port

According to the Bulletin on the State of China's Marine Environment in 2018 issued by the State Oceanic Administration of China[19], the proportions of different marine debris in monitored sea areas are shown in **Fig.3**; marine debris such as Styrofoam fragments, plastic bags, plastic bottles, and wood blocks in the seas of China accounted for more than 95% of the total marine debris.

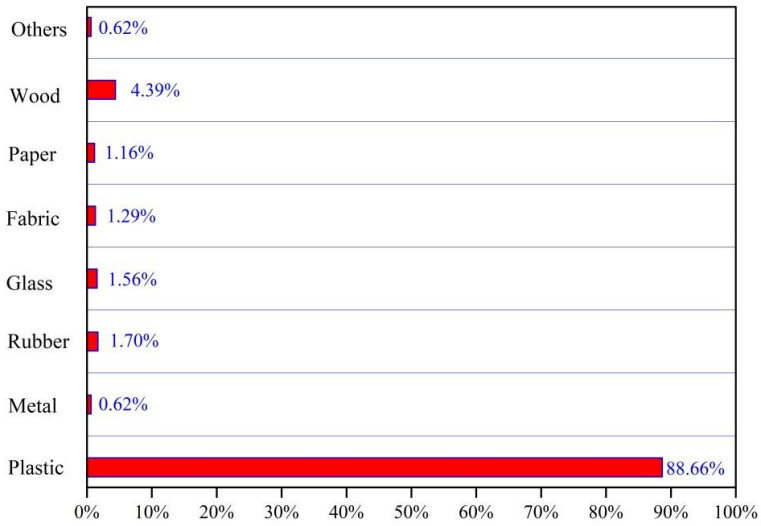

Fig.3 Proportions of marine debris in monitored sea areas[19]

According to the real marine debris' geometric statistical size, five types of marine debris are studied. The diameter of a real plastic bottle is 0.24 m, and its length is 0.4 m; the total length of a plastic bag is 1.24 m, and the width is 0.84 m; the length of a floating wood block is 1 m, the width is 0.15 m and the height is 0.15 m; the length of polystyrene foam is 0.4 m, the width is 0.4 m, and the height is 0.4 m; and the length of a blue plastic net is 0.5 m, the width is 0.4 m and the height is 0.16 m.

2.2.3 Configuration Design

According to marine debris cleaning needs of Ningbo Xiangshan Port (**Fig.4**), a new type of OSCS is proposed. The long axis of the engineering model is 500 meters in length, and the minor semi-axis is 200 meters long. In order to realize free rotation as the wind, waves, and current change, a single-point catenary mooring system is designed. Considering the geological conditions and structural strength of the OSCS, a transition buoy is installed between floating bodies and an underwater anchor chain. The general arrangement of the whole mooring system is shown in **Fig.5**, A W-type polymer polyethylene cable is adopted in the waterline plane, and a steel anchor chain is adopted in the part lying underwater. The diameters of the polymer polyethylene cable and the steel anchor chain are 64 and 38 mm, respectively.

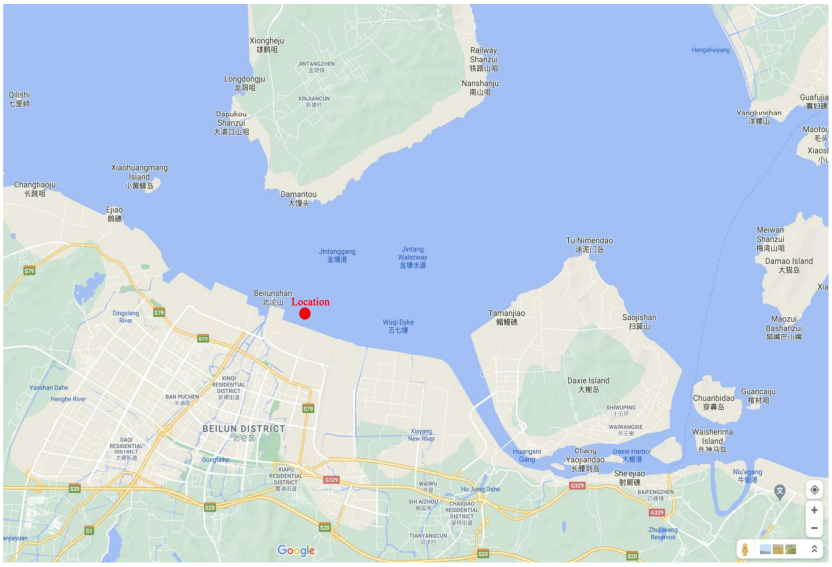

Fig.4 Location of engineering demonstration of OSCS

Tab.2 The detailed parameters of prototype OSCS

Parameter	Symbol	Value	Parameter	Symbol	Value
Length of long axis of single module equipment	*L*	500m	Diameter of main beam of permeable pontoon	*d*	0.1m
Single module equipped with minor semi-axis length	*B*	200m	Number of marine debris cleaning nets	*N*	11
Diameter of floating cylinder	*D*	2m	Length of marine debris cleaning net	*l*	40m(max)
Draft	*T*	1m	Displacement	M_T	885730kg

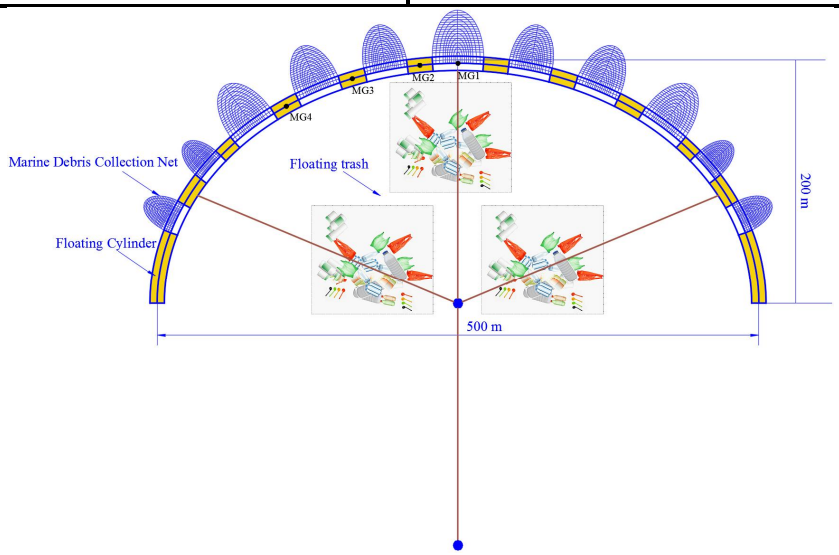

Fig.5 Arrangement of mooring system and motion gauges of OSCS

3. Experimental design

3.1 Similarity criteria

3.1.1 Similarity theory of floating body

The similarity law of naval architecture and ocean engineering structures moving in waves usually ignores the effect of viscosity, and keeps the Froude number and Strouhal number of the entity and model equal, which means that, the similarity of gravity and inertia of the two is satisfied[20]:

$$\frac{V_m}{\sqrt{gL_m}} = \frac{V_s}{\sqrt{gL_s}} \tag{1}$$

$$\frac{V_m T_m}{L_m} = \frac{V_s T_s}{L_s} \tag{2}$$

where *V*, *L*, and *T* are the speed, characteristic line scale and main period, respectively. The common physical quantities, and the stiffness coefficient, elastic coefficient, damping coefficient, wind coefficient, and flow force coefficient can be calculated by Eq.(1) and Eq.(2).

The tank test is carried out in fresh water, so the test results need to be corrected for water density. Suppose the density ratio of seawater to freshwater is γ=1.025。

In addition, the mooring system design also needs to meet the mooring system weight and weight distribution similarity law. The similarity of the elastic coefficient of the mooring system should be guaranteed-, that is, the external force and line deformation generated by the model anchor chain should be similar to the real anchor chain, and the elastic coefficient κ should be calculated according to Eq.(3).

$$\kappa = \frac{\Delta F}{\Delta l} = \frac{EA_{\mathrm{m}}}{l} \tag{3}$$

where ΔF is the change in external load acting on the anchor chain; Δl is the elongation of the anchor chain under force; EA_{m} is the axial stiffness of the mooring chain; and l is the total length of anchor chain. In this paper, the static similarity of the mooring system is guaranteed.

3.1.2 Similarity theory of flexible mesh bag

For the OSCS with a marine debris collection mesh bag, the existence of the trash collection mesh bag will affect the hydrodynamic performance of the OSCS, so the trash collection net should also meet similar conditions. There include, geometric similarity, dynamical similarity[21], mass similarity, and flexible similarity.

It is sometimes difficult to strictly scale the mesh bag completely based on the similarity theory. Therefore, in the process of making the model, other parameters of the mesh bag can be properly simplified under the condition that the stressed area of the mesh bag meets the similar requirements. In the actual test process, the simplest method is to directly use the prototype mesh bag test[21]. At this point, the diameter of the model net wire increases by λ times, the mesh number of the model mesh bag decreases by λ^2 times, the area of a single node increases by λ^2 times, and the number of nodes decreases by λ^2 times. Therefore, the total stressed area of the mesh bag in the model test can remain geometrically similar to the prototype.

For the experimental design of a OSCS model with the same mesh bag as the prototype, similar viscosity energy dissipation characteristics of the interaction between the netting and waves should be met-, that is, the criteria of the same porosity and the similar external load of the mesh bag:

$$\frac{S_s}{S_m} = 1 \tag{4}$$

$$\frac{F_s}{F_m} = \lambda_F \tag{5}$$

where S_s is the porosity of the prototype mesh bag; S_m is the porosity of the model mesh bag; F_s is the force on the prototype mesh bag; F_m is the force on the model mesh bag; and λ_F is the force similarity criterion.

This simplified method also brings some disadvantages, for example, the overall mass of the model mesh bag is large, but since the bulk density ratio of the net wire is close to 1, the mesh bag occupies a small proportion in the whole equipment when the effect of buoyancy is taken into account in the underwater test of the mesh bag, which has little influence on the test results. In addition, due to the large cable span and thickness of the prototype mesh, the force and deformation of the net were slightly different from that of the prototype in the test, and the test results were conservative.

3.2 Model test setup

3.2.1 OSCS model setup

The test was conducted at Chinese Ship Scientific Research Center. The wave tank has a total length of 69 m, a width of 46 m, and a maximum water depth of 4 m. According to the effective section size and wave-making capacity of the wave tank, the main size of the OSCS, and the required wave environment characteristics, the scale ratio of the model selected for this experiment was λ=20. The segmented model and completed test model

of OSCS are shown in **Fig.6** and **Fig.7**, respectively. According to principle of similarity, the prototype geometric parameters and model geometric parameters of OSCS are listed in **Tab.3**.

Tab.3 Main parameters of OSCS

Parameter	Symbol	Model scale	Unit
Length of long axis of single module equipment	*L*	25	m
Minor semi-axis length	*B*	10	m
Diameter of floating cylinder	*D*	0.1	m
Draft	*T*	0.05	m
Diameter of main beam of permeable pontoon	*d*	0.01	m
Number of marine debris cleaning nets	*N*	11	-
Length of marine debris cleaning nets	*l*	2(max)	m
Displacement	*MT*	108.02	kg

Fig.6 Segmented test model of OSCS

Fig.7 Completed test model of OSCS

3.2.2 Marine debris model setup

According to the actual marine debris' geometric statistical size and the principle of similarity, the five geometry parameters of marine debris and the sample size designed in the experiment are listed in **Tab.4**. The marine debris model is shown in **Fig.8**.

Tab.4 Main parameters of marine debris

Parameter	Full scale	Model scale	Unit	Sample size
Type of marine debris	5	5	--	--
Diameter of plastic bottle (middle part)	0.24	0.012	m	500
Total length of plastic bottle	0.40	0.020	m	
Total length of plastic bag	1.24	0.062	m	1000
Total width of plastic bag	0.84	0.042	m	
Length of square wood	1.00	0.050	m	500
Width of square wood	0.15	0.0075	m	
Height of square wood	0.15	0.0075	m	
Length of polystyrene foam	0.4	0.02	m	1000
Width of polystyrene foam	0.4	0.02	m	
Height of polystyrene foam	0.4	0.02	m	
Length of the blue plastic net	0.5	0.025	m	1000
Width of the blue plastic net	0.4	0.02	m	
Height of the blue plastic net	0.16	0.008	m	

(*a*) Plastic bottle

(*b*) Plastic bag

(*c*) Wood block

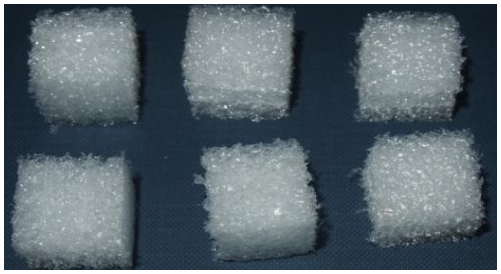

(*d*) Polystyrene foam

(e) Blue plastic net

Fig.8 Tank test model picture of marine debris

3.3 Experimental conditions

With reference to the long-term statistical law of partial wave dispersion in the target sea area, three main test variables were selected in this experiment: 1) the wave period and velocity of regular waves remained unchanged, and the influence of wave height changes on the marine debris collection efficiency was studied, as shown in **Tab.5** and **Tab.6**; 2) the wave period and wave height of regular waves remained unchanged, and the influence of flow velocity changes on marine debris collection efficiency was studied, as shown in **Tab.7**.

Tab.5 Flow velocity v=0.2236 m/s, constant period regular wave condition (1 s)

Load case	Test conditions		
	Wave high(m)	Period(s)	Wave direction(°)
A1/B1	0.025	1	0/45
A2/B2	0.035	1	0/45
A3/B3	0.050	1	0/45
A4/B4	0.100	1	0/45
A5/B5	0.150	1	0/45

Tab.6 Flow velocity v=0.2236 m/s, constant period regular wave condition (1.5 s)

Load case	Test conditions		
	Wave high(m)	Period(s)	Wave direction(°)
C1/D1	0.025	1.5	0/45
C2/D2	0.050	1.5	0/45
C3/D3	0.075	1.5	0/45
C4/D4	0.100	1.5	0/45
C5/D5	0.125	1.5	0/45
C6/D6	0.150	1.5	0/45

Tab.7 Wave height H=0.05 m, regular wave condition with constant period (1.5 s)

Load case	Test conditions		
	Flow velocity(m/s)	Period(s)	Wave direction(°)
E1/F1	0.0894	1.5	0/45
E2/F2	0.2236	1.5	0/45
E3/F3	0.2683	1.5	0/45
E4/F4	0.3578	1.5	0/45

3.4 Experimental equipment and data collection

The wave-making system of the wave tank can be used to simulate regular waves and irregular waves. The model range of regular waves was: wave height from 3 to 50 cm; period range from 0.5 to 5 s. The model range of irregular waves was: significant wave height from 3 to 40 cm, maximum wave height up to 80 cm; period from 0.5 to 3 s. The

main experiment equipment included a 6-DOF non-contact motion measurement system, a wave height meter, a gyroscope, an acceleration sensor, and a pressure sensor. The schematic diagram of the sketch of the experimental setup is shown in **Fig.9**.

According to the effective section size and wave-making capacity of the wave tank, the main size of the OSCS, and the required wave environment characteristics, the scale ratio of the model selected for this experiment was λ=20.

The 6-DOF motion of the OSCS was recorded by non-contact motion measurement system. The flow velocity was recorded by the acoustic-Doppler current meters with a high precision in measurement. The marine debris was measured by high-precision electronic scales.

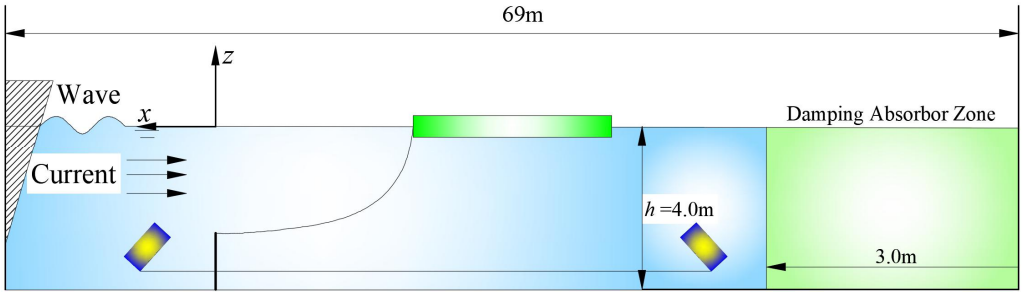

Fig.9 Sketch of the experimental setup

4. Experimental results and analysis

4.1 Study on marine debris collection efficiency

In order to quantify the trash collection efficiency of the proposed device, we define the following coefficient:

$$E = M_c / M \tag{6}$$

where E is marine debris collection efficiency, M_c is marine debris mass that enters the mesh bag, and M is total marine debris mass.

The collection efficiency of the five different types of marine debris under different load cases (A1~A5, B1~B5) with certain flow velocity, and wave period, and wave direction, and the experiments of marine debris is shown in **Fig.10**, collection efficiency curves of marine debris under different load cases are shown in **Fig.11** to **Fig.14**.

Fig.10 Experiments of marine debris collection

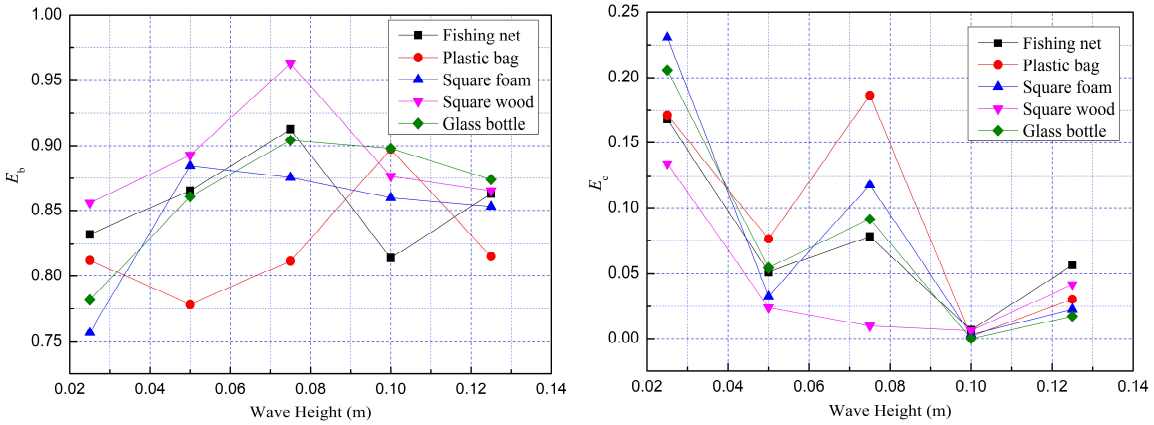

(a) Inside the mesh bag (b) Inside the U-type model but outside the mesh bag

Fig.11 Collection efficiency of marine debris (the wave period and direction are 1s, and 0°, respectively)

The marine debris collection efficiency of the mesh bag and inside the U-shaped model but outside the mesh bag under different wave heights is shown in **Fig.11**. It can be concluded that the efficiency of entering the waste mesh bag is very high. The average collection efficiency is 85.62% when the flow velocity is 0.2236 m/s, the period is 1 s, and the wave direction is 0°. It can be discovered that the collection efficiency fluctuate at 0.75 m wave height, because the initial placement position of the marine debris is not exactly the same, and thus there is a certain level of randomness. However, the overall trend of collection efficiency is an initial increase, and then a decrease afterwards with an increase in wave height. Comparing the collection efficiency curve of five different types of marine debris, it can be concluded that the collection efficiency of square blocks of wood is the highest, which is because wood density is close to half that of water's density, and so it easily enters the mesh bag.

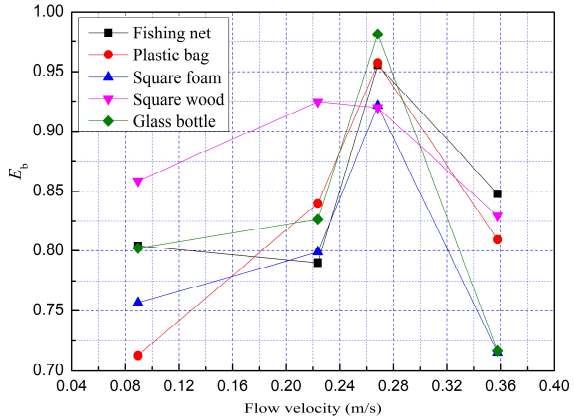

Fig.12 Collection efficiency of marine debris under different flow velocities

The marine debris collection efficiency of the mesh bag under different flow velocities is shown in **Fig.12**. According to the tank test results and the characteristics of marine debris movement, it can be found that the main influence factor of the marine

debris collection efficiency of the mesh bag is the water flow velocity, followed by wave height. The combined effect of the two factors causes the collection efficiency of marine debris to significantly increase.

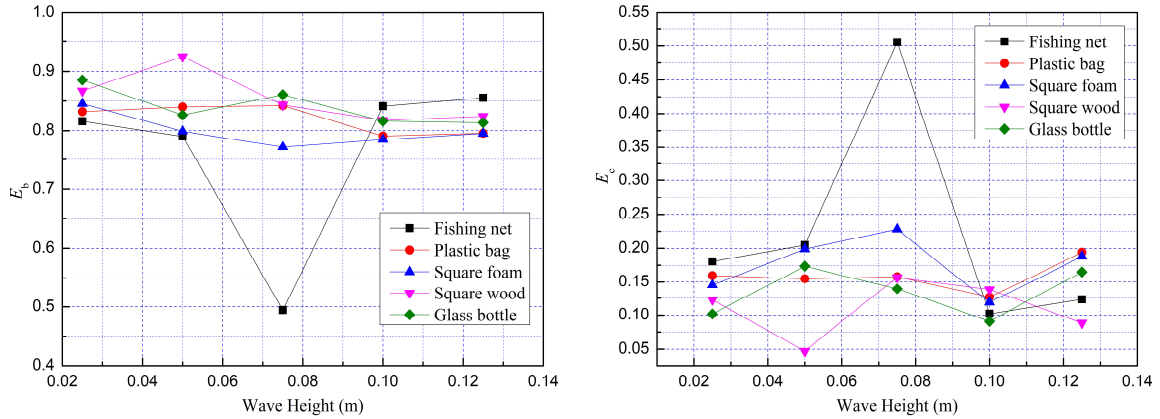

(a) Inside the mesh bag (b) Inside the U-type model but outside the mesh bag

Fig.13 Marine debris collection efficiency (the wave period and direction are 1.5 s and 0°, respectively)

According to **Fig.13**, the average collection efficiency is 81.49% when the flow velocity is 0.2236 m/s, the period is 1.5s, and the wave direction is 0°. It can be concluded that the efficiency of five different types of marine debris entering the mesh bag increases with the wave height with a certain flow velocity. The collection efficiency reaches its peak when the wave height is 0.08 m, and then the wave height increases and the collection efficiency decreases. The main reason for this is that, after increasing to 0.08 m, due to the excessive wave height, the waste will pass the OSCS under the impact of the waves, resulting in a decrease in the collection efficiency of marine debris.

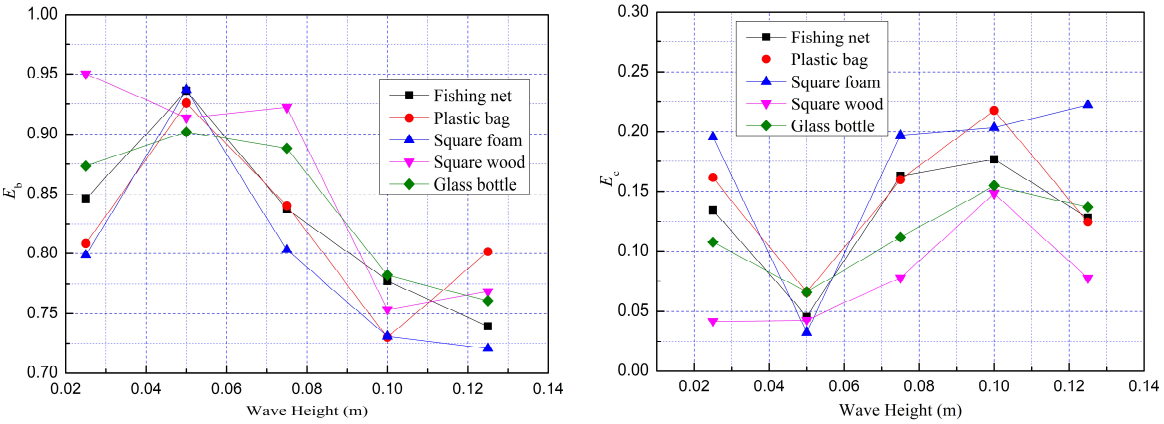

(a) Inside the mesh bag (b) Inside the U-type model but outside the mesh bag

Fig.14 Marine debris collection efficiency (the wave period and direction are 1.5 s and 45°, respectively)

The marine debris collection efficiency of the recycled mesh bag and inside the U-shaped model but outside the plastic mesh bag under different wave heights, with a wave period and direction of 1.5 s and 45°, respectively, is shown in **Fig.14**. The average collection efficiency is 82.98%. Compared with **Fig.11**, **Fig.13**, and **Fig.14**, it can be

found that the collection efficiency with a wave direction of 0° is much higher than with a wave direction of 45°, because the flow velocity direction is always 0° and there is only a steady flow in the middle 10 m area; on the other hand, as the mesh bag in the middle is the largest in size and the sizes of the mesh bags on both sides decrease gradually, some marine debris escape from both ends, and this leads to low collection efficiency. Considering the effects of combined waves and currents, wave direction has a great effect on the marine debris collection efficiency.

According to the marine debris collection efficiency curve of the marine debris entering the U-shaped floating body area but not entering the mesh bag, it can be concluded that as the wave height increases, the collection efficiency of various marine debris entering the model but not entering the mesh bag shows an overall downward trend. That is because as the wave height increases, more marine debris enters the mesh bag. Secondly, some marine debris crosses over the OSCS with the wave, which causes the collection efficiency of the U-shaped floating body model but entering the mesh bag to decrease. Comparing load cases A, B, C, and D, it can be found that the collection efficiency of various marine debris entering the mesh bag is not significantly different from the collection efficiency of marine debris entering the U-shaped floating body model but not entering the mesh bag. Therefore, the model can still provide good collection efficiency when the water surface rotates, and the model can rotate with the wave changes.

4.2 Study on hydrodynamic performance of OSCS

This section presents discussions on the hydrodynamic properties of the OSCS. A right-handed Cartesian coordinate system (geodetic coordinate system) $\boldsymbol{x} = (x, y, z)$ is fixed to above the water's surface directly to an anchor point with its negative x-direction pointing toward the middle of OSCS, its positive z-direction pointing upward, and $z = 0$ on the undisturbed free-surface. The dynamic coordinate system is fixed to the middle of the segmented floating body, and the 6-DOF motion responses are recorded based on a fixed coordinate system. The RAO motion response history curve and coverage surface area of MG1 are shown in **Fig.15** and **Fig.16**, respectively.

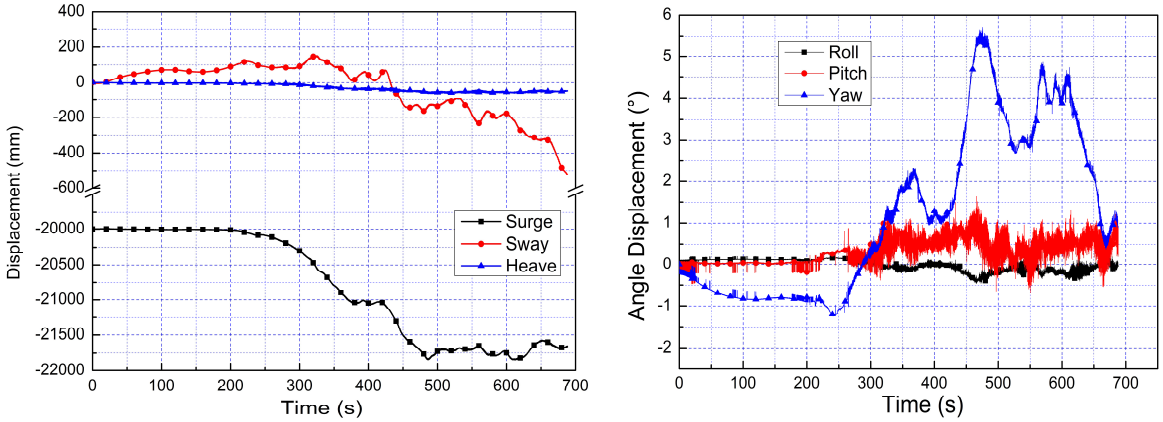

Fig.15 The 6-DOF motion response curve of MG1 under load case A1

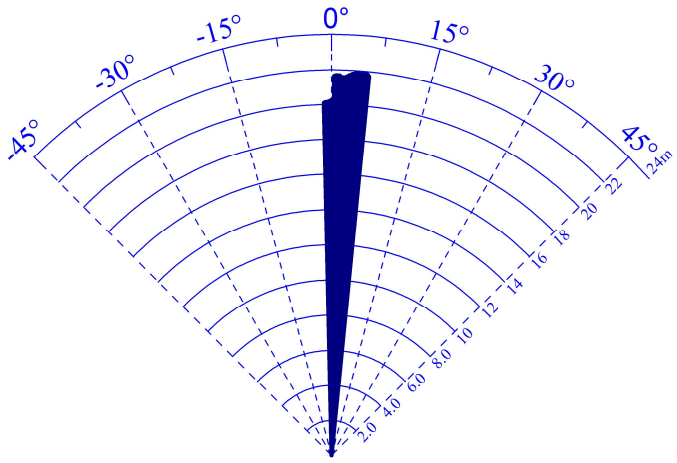

Fig.16 Coverage surface area of WG1 test point under load case A1

The RAO motion response history curve and the coverage surface area of the OSCS MG1 test point under load case A1 is shown in **Fig.15** and **Fig.16**. The motion history curve shows that the heave amplitude is the smallest (maximum is 68.92 mm), and the overall surge amplitude is the largest, while the maximum motion amplitude can reach 22 m, meaning that the OSCS can cover a large ocean surface area (**Fig.16**). Because the OSCS is a flexible body, it will be greatly deformed under the action of wind, waves, and currents. In this test, currents firstly were applied, then waves were applied after the current stability test, and as can be found in **Fig.15**, the motion was minimal in the first 200 s. The OSCS will first move with waves and currents for a period of time, and then remain stable again after the mooring system is stretched, with the motion amplitude being gradually reduced. The yaw amplitude of the OSCS is larger because it can rotate around the mooring system. The above analysis shows that the single-point mooring system of the OSCS is feasible, and the marine debris will rotate according to the wind, waves, current and its own inertial force, which helps to achieve the purpose of better marine debris collection efficiency. It can be seen from **Fig.15** and **Fig.16** that the rotational motion of the OSCS is also relatively violent, and the yaw amplitude is the

largest. The main reason for this is that we installed a cable along the longitudinal axis. The cable will contract according to the frequency and force of the wave, which causes yaw; the amplitude of roll and pitch is small under different load cases.

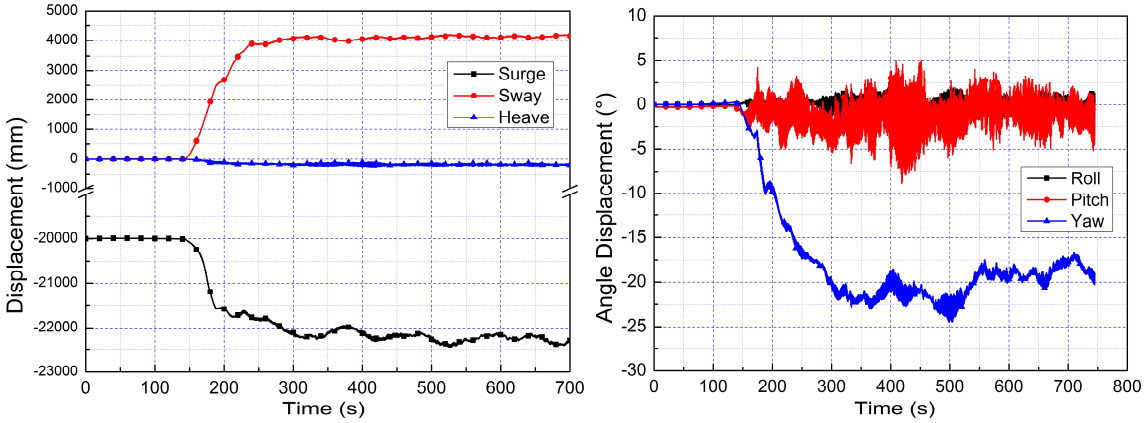

Fig.17 The 6-DOF motion response curve of MG1 under load case B4

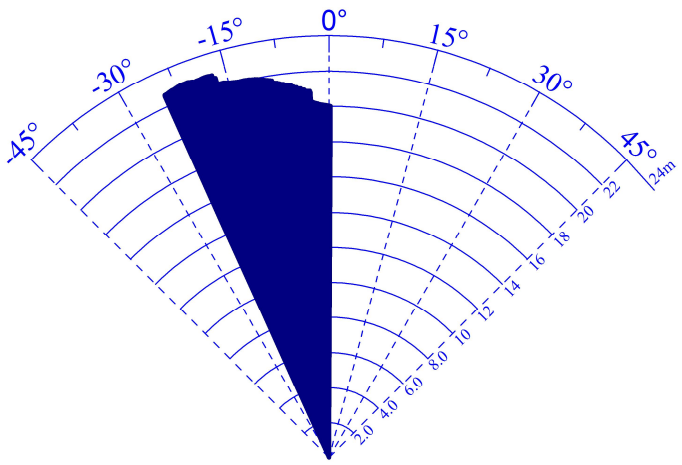

Fig.18 Coverage surface area of WG1 test point under load case B4

The difference between load case B4 and load case A1 is in the wave height and direction. In load case B4, the wave height and direction are 0.1 m, and 45°, respectively. Comparing the motion responses of load cases A1 and B4, it can be concluded that the motion amplitude and the coverage surface area of load case B4 are much larger than for load case A1. The maximum motion displacement of load case A1 is surge (1.845 m); however, that of load case B4 is sway (4.193 m). The coverage maximum angle of load case A1 is 5.319°, the load case B4 is 24.497°, and the maximum radius of coverage of load case A1 is 21.848 m, while that of load case B4 is 22.828 m. Therefore, it can be found that the novel OSCS can cover a large ocean surface area. It can be found from **Fig.18** that the OSCS deformation increases with the increase in rotation angle, but has two jump turns at 4° and 17°.

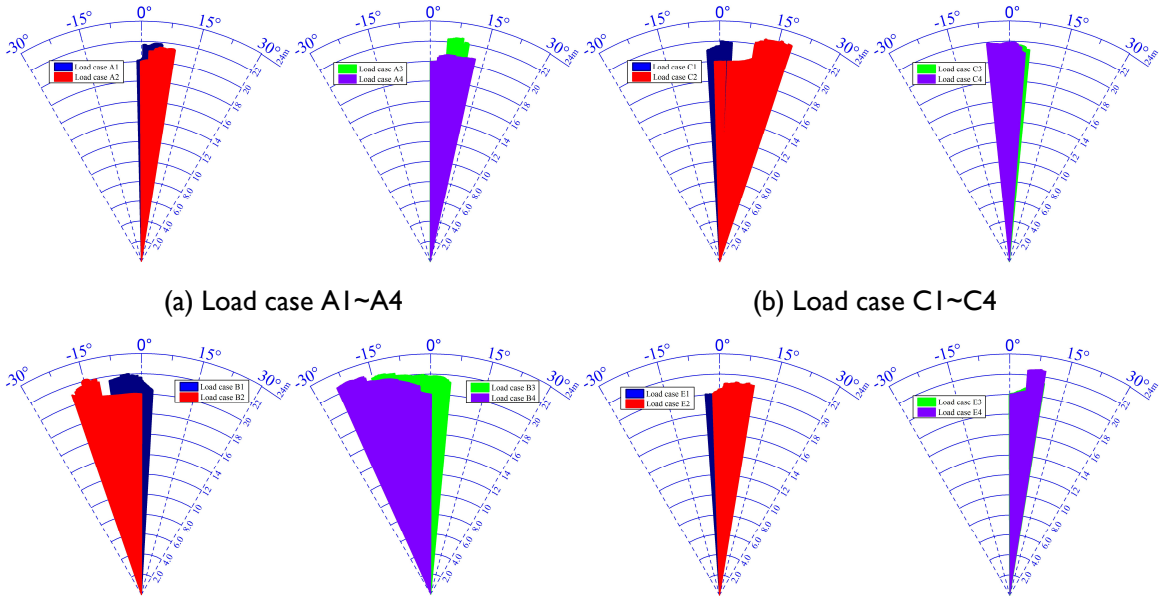

(a) Load case A1~A4 (b) Load case C1~C4

(c) Load case B1~B4 (d) Load case E1~E4

Fig.19 Coverage surface area of WG1 test point under different load cases

The coverage surface areas of the WG1 test point under different load cases are shown in **Fig.19**; load cases A1 to A4 with different wave height, load cases A and C with different periods, load cases A and B with different wave direction, load cases E1 to E4 with different flow velocity. Comparing **Fig.19a,b**, it can be discovered that motion response is greatest when wave height is 0.05 m, rather than 0.075 m or 0.1 m, which is because the OSCS has a draught of 0.05 m. So, the motion response of OSCS has a non-monotone variation with an increase in wave height. Comparing load cases A, B, C, and E, it can be concluded that the rotation of the OSCS has a good effect, and it can be used to clean a large ocean surface at high efficiency. According to analysis coverage surface area of the WG1 test point, the rotation angle is 6°~15° when the wave direction is 0°, while the rotation angle is 15°~30° when the wave direction is 45°. Comparing load cases E1 and E4, it can be concluded that the motion response of OSCS increases with an increase in flow velocity, but the coverage surface area is reduced with an increase in flow velocity with a certain wave height and wave direction.

5. Conclusions

This paper proposed new type of effective ocean surface cleaning system (OSCS). The marine debris collection efficiency and hydrodynamic performance of the OSCS were studied by a series of model tests. According to the test results, the following conclusions are drawn:

1) The test results show that the average collection efficiency was 85.62% under load case A**,** the average collection efficiency was 64.87% under load case B, the average

collection efficiency is 81.49% under load case C, and the average collection efficiency was 82.98% under load case D**.** According to the test results and the characteristics of trash movement, it was found that the main influence factor on the marine debris collection efficiency is the current velocity, and the second is the wave height.

2) According to the analysis of the coverage surface area of the WG1 test point, the rotation angle is 6°~15° when the wave direction is 0°, while the rotation angle is 10°~30° when the wave direction is 45°. The motion response of OSCS increases with an increase in flow velocity, but the coverage surface area is reduced with an increase in flow velocity with a certain wave height and wave direction. The motion response is greatest when wave height is 0.05 m in this test, which is a non-monotone variation with an increase in wave height.

3) Compared with the traditional marine debris cleaning equipment, the marine debris collection efficiency of the OSCS proposed in this paper was higher, the amount of trash collected at one time is large, and it is effective for different types of marine debris; because the main pontoon adopts a flexible design, the equipment can still work well under the action of large waves, and the manufacturing process of the whole attached model is simple.

4) OSCS can be arranged at fixed points through the mooring system, which was suitable for the marine debris accumulation zone in open sea areas. OSCS has mobility, and different sea area layouts could be realized through mooring system, which have automatic collection features. Through comparison with the status of domestic and foreign research status, we can conclude that the OSCS has strong innovation and engineering application prospects.

Reference

[1]. Rochman C M, Browne M A, Halpern B S, et al. Classify plastic waste as hazardous[J]. Nature, 2013, 494(7436): 169-171.

[2]. Europe P. An analysis of European plastics production, demand and waste data[J]. Plastics–the facts, 2015: 147.

[3]. Walpole S C, Prieto-Merino D, Edwards P, et al. The weight of nations: an estimation of adult human biomass[J]. BMC public health, 2012, 12(1): 1-6.

[4]. Carpenter E J, Smith K L. Plastics on the Sargasso Sea surface[J]. Science, 1972, 175(4027): 1240-1241.

[5]. Wong C S, Green D R, Cretney W J. Quantitative tar and plastic waste distributions in the Pacific Ocean[J]. Nature, 1974, 247(5435): 30-32.

[6]. Jambeck J R, Geyer R, Wilcox C, et al. Plastic waste inputs from land into the ocean[J]. Science, 2015, 347(6223): 768-771.

[7]. Merkl A, Stuchtey M, Russel S, et al. Stemming the Tide: Land-based strategies for a plastic-free ocean[J]. Ocean Conservancy and McKinsey Center for Business and Environment, 2015, 48.

[8]. Wilcox C, Van Sebille E, Hardesty B D. Threat of plastic pollution to seabirds is global, pervasive, and increasing[J]. Proceedings of the National Academy of Sciences, 2015, 112(38): 11899-11904.

[9]. Yi Z, Chen D, Yang J, et al. Review of floating waste recovery methods[C].// 2017 Proceedings of the 18th China Marine (Coastal) Engineering Symposium. 2017:752-756.

[10]. https://www.wasteshark.com/#about.

[11]. Ruangpayoongsak N, Sumroengrit J, Leanglum M. A floating waste scooper robot on water surface[C]//2017 17th International Conference on Control, Automation and Systems (ICCAS). IEEE, 2017: 1543-1548.

[12]. Wang Z, Liu Y, Yip H W, et al. Design and hydrodynamic modeling of a lake surface cleaning robot[C]//2008 IEEE/ASME International Conference on Advanced Intelligent Mechatronics. IEEE, 2008: 1343-1348.

[13]. Zhang H T, Cao J B, Cao J X, et al. Design for the Multi-functional Floating Garbage Disposal Device[C]//2nd Annual International Conference on Advanced Material Engineering (AME 2016). Atlantis Press, 2016: 1299-1304.

[14]. https://theoceancleanup.com /rivers/.

[15]. https://theoceancleanup.com/milestones/system001/

[16]. http://www.omae2020.com/.

[17]. Huang Y, Yuan Z M, Dai S S, et al. Plastic Debris in Waves: An Experimental Study[C]//The 30th International Ocean and Polar Engineering Conference. International Society of Offshore and Polar Engineers, 2020.

[18]. http://www.bianbao.net/

[19]. State Oceanic Administration. China's State Oceanic Environment Bulletin 2018.

[20]. Jianmin Yang, Longfei Xiao, Zhenbang Sheng. Experimental study on the hydrodynamics of Marine engineering [M]. Shanghai: Shanghai Jiao Tong University Press, 2008.

[21]. Gui Fu-kun, Li Yu-cheng, Zhang Huai-hui. The proportional criteria for model testing of force acting on fishing cage net[J]. China Offshore Platform, 2002, 17(9):22-25.